

Spatiotemporal few-photon optical nonlinearities through linear optics and measurement

K. J. Resch

Institut für Experimentalphysik, Universität Wien, Boltzmannngasse 5, 1090 Vienna, Austria

(Received 2 July 2004; published 24 November 2004)

It is well known that optical nonlinearities are extremely weak at the quantum, or single-photon, level. This has been one of the major difficulties for optical implementations of universal, scalable quantum computation. Knill, Laflamme, and Milburn [Nature (London) **409**, 46 (2001)] showed, among other things, that one could perform the elusive two-qubit logic gates with only linear-optical elements if one also uses extra single photons and measurement. In this work, we apply linear-optics techniques to produce effects in few-photon beams that are more familiar to strong-field nonlinear optics. Specifically, we show that these methods are sufficient to change the spatial (or temporal) properties of a light beam with strong dependence on its constituent number of photons; such phenomena cannot occur via linear optics alone.

DOI: 10.1103/PhysRevA.70.051803

PACS number(s): 42.50.Dv, 03.67.-a, 42.65.-k

Photons interact with each other notoriously weakly. This fact has been one of the main stumbling blocks for optical implementations of two-qubit, entanglement-changing, quantum logic gates requisite for quantum information processing. Atoms can mediate effective interactions between photons through nonlinear optical effects, although these too are extremely weak at the quantum level. Proposals and methods for attacking this problem were based on enhancing these existing, but weak, optical nonlinearities via cavity QED [1], quantum interference [2], photon-exchange interactions [3], and electromagnetically induced transparency [4]. More recently, Knill, Laflamme, and Milburn (KLM) shocked the quantum optics community when they showed that two-qubit quantum logic operations could be produced using only *linear* optical elements supplemented with extra single photons and by conditioning the evolution on specific measurement outcomes [5]. Since then, much more work has been done to simplify, understand, and realize these effects [6–8]. In addition, linear optics techniques have been applied to such problems as producing “high-noon” states [9], performing QND measurements [10], and making “quantum filter” devices [11]. But the kinds of effects and applications thus far rely on only the nonlinear amplitude or phase evolution linear optics methods can induce. Traditional strong-field nonlinear optics has demonstrated that striking nonlinear effects can also appear in the spatial or temporal properties of optical beams; well-known examples include self-focusing, or temporal and spatial soliton formation. For most applications in quantum optics, it is desirable to work within a single-mode picture since interference is maximized and decoherence is minimized. However, as we will show in this work, spatial nonlinear optical effects can be probabilistically generated through linear optics and projective measurement using *imperfectly overlapping* optical modes. (The effects worked out explicitly here in the spatial domain have direct temporal analogues due to similar dependence on space and time in the field operators and quantum states.) The first signature of these spatial nonlinearities is that photon-number states can conditionally evolve to pure states with the same number of photons, but very different beam intensity profiles.

Consider the situation shown in Fig. 1. A Gaussian beam

containing n -independent (uncorrelated) photons in mode 1 is incident on a beam splitter with reflection amplitude r . We will refer to these photons as simply “beam” photons. A single, “ancilla,” photon is incident on the same beam splitter from the other side in mode A . Mode B passes through a spatial mode filter that separates light into spatial mode F and the set of all modes orthogonal to F (simply labeled \bar{F}). Both of these new beams terminate at ideal single-photon counting detectors. We consider the properties of the new state in mode 2 in those cases in which *exactly* one photon is detected in mode F and no photons are detected in \bar{F} .

The initial state of the beam ancilla, $|\Psi_n\rangle$, is the tensor product of the n -photon state in mode 1 and the single photon in mode A ,

$$\begin{aligned}
 |\Psi_n\rangle = & \frac{1}{\sqrt{n!}} \int \cdots \int dk_1 dk_2 \cdots dk_n f_1(k_1) \\
 & \times f_1(k_2) \cdots f_1(k_n) a_1^\dagger(k_1) a_1^\dagger(k_2) \cdots a_1^\dagger(k_n) \\
 & \times \int dk_A f_A(k_A) a_A^\dagger(k_A) |0\rangle, \quad (1)
 \end{aligned}$$

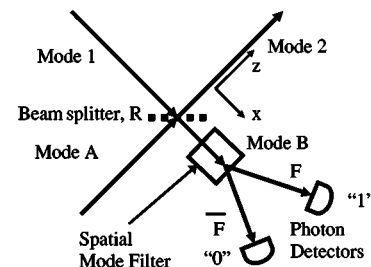


FIG. 1. Method for producing spatial nonlinear optical effects at the few-photon level via linear optics and projective measurement. An N -photon state and a one-photon state are incident on a beam splitter of reflectivity R . These incident modes do not, in general, have the same beam shapes. A spatial filter is used to separate output mode B photons into a single spatial mode F and all other spatial modes that are orthogonal to F , labeled \bar{F} . The state of interest in mode 2 is produced conditional on having exactly one photon in mode F and no photons in \bar{F} .

where $f_1(k)$ describes the mode function for each beam photon, $f_A(k)$ describes the normalized mode function for the ancilla photon, and $a_{1(A)}^\dagger$ are the raising operators for mode 1(A). Both mode functions are chosen such that $\int dk f^*(k)f(k)=1$, which ensures the state is properly normalized. In this theoretical treatment, we consider the case where all photons are monochromatic but spatially localized. Under these conditions, the nonlinear effects can only be spatial; temporal nonlinear effects require that the beam and ancilla photons have different temporal modes. The beam-splitter reflection and transmission amplitudes, r and t , are constant, real (the phases will be included in the mode transformation), and the beam splitter is lossless ($r^2+t^2=1$). We write the action of the beam splitter in terms of the field operators as $a_1^\dagger \rightarrow ta_B^\dagger + ra_2^\dagger$, $a_A^\dagger \rightarrow ra_B^\dagger - ta_2^\dagger$, where $a_{2(B)}^\dagger$ are the raising operators for mode 2(B). The beam splitter transforms the state according to

$$|\Psi_n\rangle \rightarrow \frac{1}{\sqrt{n!}} \int \dots \int dk_1 \dots dk_n f_1(k_1) \dots f_1(k_n) [ra_B^\dagger(k_1) + ta_2^\dagger(k_1)] \dots [ra_B^\dagger(k_n) + ta_2^\dagger(k_n)] \int dk_A f_A(k_A) [ra_B^\dagger(k_A) - ta_2^\dagger(k_A)] |0\rangle. \quad (2)$$

The spatial mode filter separates only the spatial mode F defined by the mode function $f_F(k)$. (For temporal nonlinear effects, postselection of a single temporal mode is required). By postselecting only those cases where exactly one photon was detected in mode F and no photons were detected in \bar{F} , we describe a projective measurement onto the state $\int dk f_F(k) a^\dagger(k) |0\rangle$. Only two amplitudes contribute to the post-selected final state—all $n+1$ photons are reflected or two photons are transmitted and $n-1$ photons are reflected. The conditional evolution of the n beam photons is

$$|n\rangle_1 \rightarrow \frac{1}{\sqrt{n!}} \int dk_1 \int dk_2 \dots \int dk_n f_1(k_1) f_1(k_2) \dots f_1(k_{n-1}) r^{n-1} \times \left[r^2 f_1(k_n) \int dk_A f_F^*(k_A) f_A(k_A) - nt^2 f_A(k_n) \right. \\ \left. \times \int dk_A f_F^*(k_A) f_1(k_A) \right] a_2^\dagger(k_1) a_2^\dagger(k_2) \dots a_2^\dagger(k_n) |0\rangle, \quad (3)$$

where we have not renormalized. Note that this final state still contains n photons. Many of the interesting nonlinear optical properties of the final state come from its dependence on the photon number, n . Physically, this n arises from the n ways in which one of the beam photons was detected. On the other hand, there was only a single path where all $n+1$ photons were reflected from the beam splitter and the ancilla photon was detected—thus this term is not multiplied by n . The ratio of these two interfering amplitudes changes as one changes the beam photon number making beam characteristics photon-number dependent. If we consider the single-mode case, i.e., $f_1(k)=f_F(k)=f_A(k)$, then Eq. (3) reduces to $|n\rangle_1 \rightarrow \sqrt{R^{n-1}} [R - n(1-R)] |n\rangle_2$, in which we have substituted the reflection probability for the reflection amplitude, $R=r^2$.

This expression has been used to describe the evolution of the nonlinear sign-shift operation [8,12].

To show some explicit features of nonlinear state evolution, we calculate the rms width of the resultant beam intensity distribution created in mode 2 at the beam splitter as a function of the incident number of photons in mode 1. For the purposes of this calculation, the light propagates along the z direction. We assume that the light is spatially localized in the x direction, but infinite in extent in the y direction; this creates an effective two-dimensional beam since the y evolution will contribute only a global phase. We model the incident photon and ancilla photon mode functions as Gaussians with waists at the beam splitter; these functions can be written as $f(k_x, \sigma) = [(2/\pi)\sigma^2]^{1/4} \exp(-k_x^2 \sigma^2)$, where k_x are the transverse wave vectors and σ is the rms width of the intensity distribution along the x direction (in general, σ is different for the incident, ancilla, and filter modes). We treat the monochromatic case so that the magnitude of the total wave vector $|\vec{k}| = \sqrt{k_x^2 + k_y^2 + k_z^2}$ is constant. The normalization constant here is important for calculating the overlap of the mode functions. In these calculations, we choose the filter mode to be identical to the ancilla mode, i.e., $\int dk_A f_F^*(k_A) f_A(k_A) = 1$. These mode overlap integrals control the weighting of the two amplitudes in the final state, but even with this constraint, any weighting of the amplitudes can be achieved using the beam-splitter reflectivity.

Following quantum optics theory [13], we write the expectation value of the intensity as $\langle I(\mathbf{r}, t) \rangle_2 = \langle \psi |_2 \hat{E}^-(\mathbf{r}, t) \hat{E}^+(\mathbf{r}, t) | \psi \rangle_2$, where $\hat{E}^+(\mathbf{r}, t) = 1/\sqrt{2\pi} \int d\mathbf{k} \int d\omega \exp(i\mathbf{k} \cdot \mathbf{r} - i\omega t) \hat{a}(\mathbf{k}, \omega)$ and $\hat{E}^-(\mathbf{r}, t) = 1/\sqrt{2\pi} \int d\mathbf{k} \int d\omega \exp(-i\mathbf{k} \cdot \mathbf{r} + i\omega t) \hat{a}^\dagger(\mathbf{k}, \omega)$, where \mathbf{r} is the position, \mathbf{k} is the wave vector, ω is the frequency, and we have dropped the polarization. These operators can be considerably simplified for the calculations of interest here using the constraints we have imposed. Since our incident wave packets are monochromatic and plane waves in the y direction, the frequency component and k_y component of the operators contribute a meaningless, overall phase. For now, we consider only the intensity at $z=0$ (at the beam splitter), which removes the k_z dependence, and $\hat{E}^+(x) = 1/\sqrt{2\pi} \int dk_x \exp(ik_x x) \hat{a}(k_x)$ and $\hat{E}^-(x) = 1/\sqrt{2\pi} \int dk_x \exp(-ik_x x) \hat{a}^\dagger(k_x)$.

Figures 2(a) and 2(b) show the results of a specific set of normalized intensity calculations for one- (solid line), two- (long-dashed line), three- (short-dashed line), and four-photon (dotted line) states. These intensities were calculated for an incident beam rms width of 100 μm and a smaller, but comparable, ancilla width of 75 μm . Figure 2(a) illustrates the behavior in the perturbative limit where the beam-splitter reflectivity is high, $R=83\%$. In this limit, the amplitude for all $n+1$ photons to have been reflected is dominant but the interfering term is non-negligible and grows in significance with the photon number n . The widths of the intensity distributions can easily be seen to increase with increasing initial (and therefore final) photon number; the rms widths are, for increasing photon number, 107, 109, 113, and 124 μm . The operation creates a photon-number-dependent beam expansion. In Fig. 2(b), the beam-splitter reflectivity has been de-

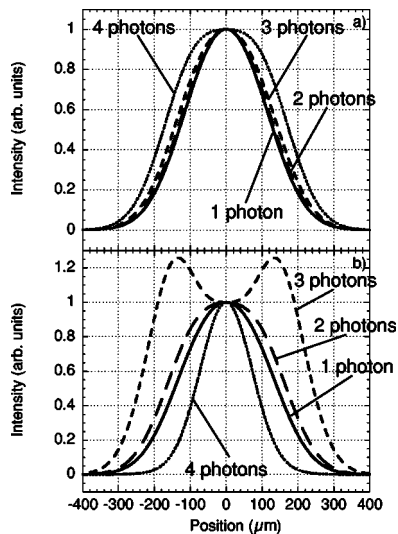


FIG. 2. Two specific examples of conditional beam intensities for one-, two-, three-, and four-photon states at the beam-splitter output. Normalized intensity predictions as a function of position are shown and were produced using the correlation function method described in the text. An input N -photon state with intensity rms width $100 \mu\text{m}$ and an ancilla photon with rms intensity width $75 \mu\text{m}$ were mixed at a beam splitter with reflection probability (a) $R=83\%$ and (b) $R=76\%$. In (a), the rms width of the outgoing beam increases with increasing photon number—higher photon-number states expand more than lower. In (b) we move beyond this perturbative limit and the widths obey no such simple trend. Beam distortion is very apparent for the three-photon state due to strong destructive interference.

creased to $R=76\%$. In this case, the intensity profiles depend very strongly on the photon number, but the simple perturbative trend is no longer present. One can also see that this method can lead to significant beam profile distortion. This is especially apparent near maximum destructive interference as is the case, under these conditions, for the three-photon state.

In Fig. 3, we summarize the widths of the postselected output states as a function of the beam-splitter reflectivity for cases where the input state has a fixed width of $100 \mu\text{m}$ and the ancilla photon has rms width (a) 20, (b) 75, (c) 125, and (d) $500 \mu\text{m}$. In the limit as $R=1$, all of the beams have a width of $100 \mu\text{m}$ (and, in fact, all beam shapes are identical). In this limit, the beam splitter is a perfect mirror which reflects all input photons to the output and the ancilla to the spatial filter and detector. In the opposite limit, as $R \rightarrow 0$, there is strong dependence of the width on the photon number. In this limit, the dominant contribution to the final state comes from the amplitude for two photons to be transmitted and $n-1$ photons to be reflected. The number dependence originates from an averaging of the mode sizes of the beam and ancilla photons. In this limit for the one-photon state, the outgoing photon is the ancilla and therefore its width is equal to the ancilla width. As the photon number is increased, the outgoing intensity width trends towards that of the beam (i.e., $100 \mu\text{m}$).

In Figs. 3(b) and 3(c), the ancilla photon width is chosen to be slightly smaller and slightly larger, respectively, than the beam photons. In these figures, as is typical when the beam and ancilla mode sizes are similar, rapid variations occur in the beam width, from much broader than the initial beam to narrower, for certain reflectivities that increase with increasing photon number. These width “resonances” occur near the maximum destructive interference between the two interfering processes. Since the modes do not match perfectly, good destructive interference can be either set up in the center of the beam, in which case the resultant beam is broadened, or in the tails of the beam, in which case it is narrowed. Although it is not shown explicitly, the resonances become narrower as the beam and ancilla modes become more similar. The resonances for n -photon states occur at approximately $R=n/(n+1)$, which, in the case of perfect mode matching, corresponds to the condition for maximum destructive interference in a generalized Hong-Ou-Mandel-style interferometer [8,14]. Note also that the maxima and minima of the resonances decrease with increasing photon

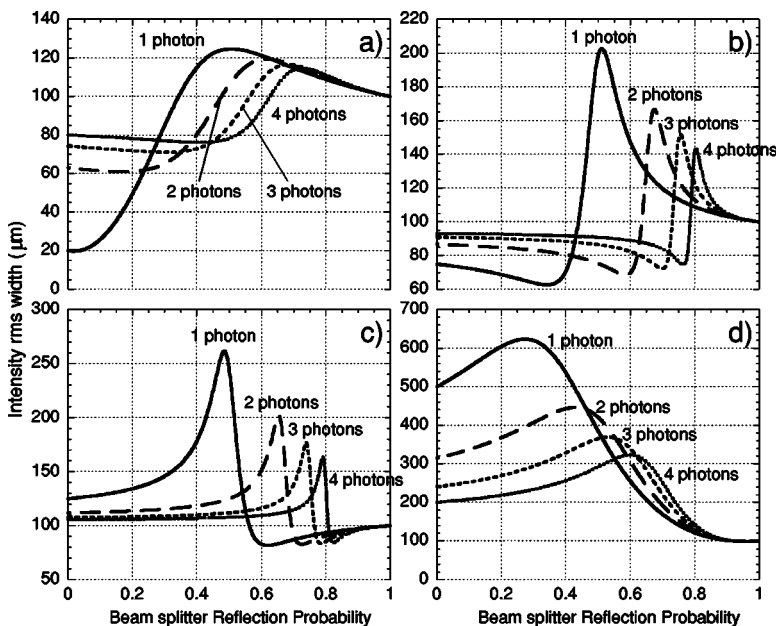


FIG. 3. Intensity width vs beam-splitter reflection probability. For incident one-, two-, three-, and four-photon states with initial rms widths of $100 \mu\text{m}$, the rms width of the outgoing conditional intensity is shown as a function of the beam-splitter reflectivity for ancilla widths (a) 20, (b) 75, (c) 125, and (d) $500 \mu\text{m}$. The behavior in the limits as $R=1$ and $R \rightarrow 0$, the high reflectivity perturbative behavior, and the rapid, photon-number-dependent changes in the width are discussed in the text. The most important feature, however, is that the conditional intensity profiles are very different for different photon-number states. Such number-dependent beam profiles cannot occur with linear optics alone.

number. In Eq. (3), very roughly speaking, there are $n-1$ beam photons in the output state and the n th photon that is in a superposition. Thus, similar to the behavior in the limit as $R \rightarrow 0$, the strong broadening or narrowing of the n th photon is washed out by the unaffected $n-1$ other photons.

In Fig. 2(a), where the ancilla mode had a width of $75 \mu\text{m}$ [same as in Fig. 3(b)], we pointed out that in the high reflectivity limit, the beam width became broader with increasing photon number. In the same limit, in Fig. 3(c), where the ancilla mode is slightly larger than the beam mode, the beam is compressed more with increasing photon number. These trends also hold for the high R limit for Figs. 3(a) and 3(d), although they are not visible on the displayed scale. With a narrower ancilla mode, there is more destructive interference in the center of the beam tending to make the beam broader; for a broader ancilla mode, there is more destructive interference in the tails of the beam tending to make the beam narrower. In addition, the smaller amplitude (i.e., the I^{2n-1} amplitude) is enhanced by a factor of the photon number n making the expansion or compression more pronounced for higher photon number states.

These measurement-based nonlinearities are necessarily probabilistic since one considers only those cases where a specific outcome is observed—in this case, detection of one photon in mode F and none in \bar{F} . In the examples discussed here, the probability for the desired detection depends strongly on the parameters under consideration. Most significantly, the desired outcome probability is highly suppressed near the width resonances due to strong destructive interference. However, since the modes are not perfectly overlapping, this interference is never perfect and any point on the curve can occur with some probability. Conversely, in the high reflectivity limit, the probability of obtaining the desired measurement outcome can be very high and still show significant broadening or compression. Experimentally, it is beyond current technology to reliably measure one and only one photon in a given spatial mode once realistic loss and

detection efficiencies are considered. That being said, the effects described in this work for one and two photons should be observable with current parametric down-conversion sources and multiphoton coincidence postselection. Such techniques have already proven sufficient for demonstrating two-qubit quantum logic and two-photon nonlinearities in lossy single-mode linear optics experiments with real single-photon counting detectors [7,8].

Nonlinear optical interactions mediated by higher-order atomic susceptibilities are extremely weak at the quantum level. KLM showed how the act of measurement, which is routine in the laboratory, and the use of single-photon sources could create effective interactions between photon pairs useful for two-qubit quantum gates. We have shown that these techniques have promise outside the realm of quantum information processing. Photon-number-dependent spatial or temporal properties can be created in a light beam via these same techniques when one uses beam and ancilla photons in different spatial or temporal modes. There is a large range of possible applications for such a general approach, including the generation of photon-photon bound states [15] and nonlinear beam propagation and focusing. It is often the case that new physics lie at the borders of existing research fields. By using cutting-edge methods for quantum computation and more traditional approach quantum coherence and interference, many classic nonlinear optical effects, normally constrained to the high-field domain, may be extendible to the few-photon level.

The author is grateful to Kaoru Sanaka, Aephraim Steinberg, Morgan Mitchell, Jeff Lundeen, and Gabriel Molina-Terriza for stimulating discussions that shaped the direction of these ideas. This work was supported by ARC Seibersdorf Research GmbH, the Austrian Science Foundation (FWF), Project No. SFB 015 P06, NSERC, and the European Commission, Contract No. IST-2001-38864 (RAMBOQ).

-
- [1] Q. A. Turchette *et al.*, Phys. Rev. Lett. **75**, 4710 (1995); A. Rauschebeutel *et al.*, *ibid.* **83**, 5166 (1999).
- [2] K. J. Resch, J. S. Lundeen, and A. M. Steinberg, Phys. Rev. Lett. **87**, 123603 (2001); **89**, 037904 (2002).
- [3] J. D. Franson, Phys. Rev. Lett. **78**, 3852 (1997).
- [4] S. E. Harris and L. V. Hau, Phys. Rev. Lett. **82**, 4611 (1999); M. M. Kash *et al.*, *ibid.* **82**, 5229 (1999).
- [5] E. Knill, R. Laflamme, and G. Milburn, Nature (London) **409**, 46 (2001).
- [6] T. B. Pittman, B. C. Jacobs, and J. D. Franson, Phys. Rev. A **64**, 062311 (2001); T. C. Ralph *et al.*, *ibid.* **65**, 012314 (2001); T. Rudolph and J.-W. Pan, quant-ph/0108056 (2001); T. C. Ralph *et al.*, Phys. Rev. A **65**, 062324 (2002); G. G. Lapaire *et al.*, *ibid.* **68**, 042314 (2003).
- [7] T. B. Pittman *et al.*, Phys. Rev. A **68**, 032316 (2003); J. L. O'Brien *et al.*, Nature (London) **426**, 264 (2003); S. Gasparoni *et al.*, Phys. Rev. Lett. **93**, 020504 (2004).
- [8] K. Sanaka, T. Jennewein, J.-W. Pan, K. Resch, and A. Zeilinger, Phys. Rev. Lett. **92**, 017902 (2004).
- [9] H. Lee, P. Kok, N. J. Cerf, and J. P. Dowling, Phys. Rev. A **65**, 030101 (2002); J. Fiurasek, *ibid.* **65**, 053818 (2002); M. W. Mitchell, J. S. Lundeen, and A. M. Steinberg, Nature (London) **429**, 161 (2004).
- [10] P. Kok, H. Lee, and J. P. Dowling, Phys. Rev. A **66**, 063814 (2002); G. J. Pryde *et al.*, Phys. Rev. Lett. **92**, 190402 (2003).
- [11] H. F. Hoffmann and S. Takeuchi, Phys. Rev. Lett. **88**, 147901 (2002).
- [12] H. F. Hoffmann and S. Takeuchi, e-print quant-ph/0204045.
- [13] R. J. Glauber, in *Quantum Optics and Electronics*, edited by C. DeWitt, A. Blandin, and C. Cohen-Tannoudji (Gordon and Breach, New York, 1965) pp. 63–185.
- [14] C. K. Hong, Z. Y. Ou, and L. Mandel, Phys. Rev. Lett. **59**, 2044 (1987).
- [15] R. Y. Chiao, I. H. Deutsch, and J. C. Garrison, Phys. Rev. Lett. **67**, 1399 (1991).